 CMES, vol.81, no.3, pp.249-267, 2011

Unified Dispersion Characteristics of Structural Acoustic Waveguides

Abhijit Sarkar[1], **M. V. Kunte**[2] **and Venkata R. Sonti**[2]

Abstract: In this article, we show with some formalism that infinite flexible structural acoustic waveguides have a general form for the dispersion equation. The dispersion equation of all such waveguides should conform to a generic form. This allows us to bring out the common features of structural acoustic waveguides. We take three examples to demonstrate this fact, namely, the rectangular, the circular cylindrical and the elliptical geometries. Where necessary, the equations are simplified for applicability to a particular frequency-regime before demonstrating the conformance to the generic form of the dispersion relation. It is then shown that the coupled wavenumber solutions of all these systems can be represented on a single schematic.

Keywords: structural acoustic waveguide, dispersion characteristics, unification

1 Introduction

Recently, several studies were presented on the dispersion characteristics of waveguides (with rectangular, circular cylindrical and elliptic cylindrical geometries) using the asymptotic methods by Sarkar and Sonti (2007a,b,c,d, 2009a,b) and Kunte, Sarkar, and Sonti (2010). Despite the geometrical differences amongst the systems, there seems to be an underlying feature common to these waveguides in the manner in which the uncoupled structural and acoustic waves form coupled waves. In this article, we intend to bring out this feature by presenting the coupled dispersion equation for the different geometries in a generic form. And along with this generic equation is presented a generic solution of the coupled waves in a schematic onto which all the coupled wavenumbers for the different geometries can be superposed.

The structural acoustic systems that are considered are as follows : -

[1] Department of Mechanical Engineering, Indian Institute of Technology Madras, Chennai - 600036, India

[2] Vibro-Acoustics Lab, Facility for Research in Technical Acoustics, Department of Mechanical Engineering, Indian Institute of Science, Bangalore - 560012, India

1. The two-dimensional structural acoustic waveguide consisting of (a) a fluid column supported on a flexible plate with a rigid plate at the top (b) a fluid column supported by a flexible plate with zero pressure at the top. (see figure 1a).

2. The fluid-filled circular cylindrical shell. Results of this problem are presented separately for the different circumferential modes as follows (a) the axisymmetric mode ($n = 0$) (b) the beam mode ($n = 1$) (c) the higher order modes ($n > 1$). (see figure 1b).

3. The fluid-filled elliptic cylindrical shell. (see figure 1c).

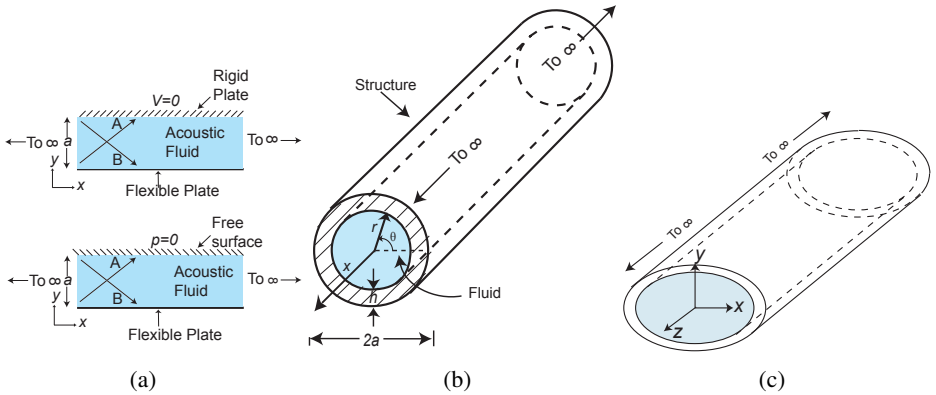

(a) (b) (c)

Figure 1: Structural acoustic waveguide systems studied in this article : (a). Two dimensional rectangular waveguide, (b). Fluid-filled circular cylindrical shell, (c). Fluid-filled elliptical cylindrical shell.

It will be shown that for each of these systems the coupled dispersion relation has the following generic form

$$f_1 f_2 p \pm \mu f_3 f_4 = 0, \tag{1}$$

where μ is the fluid-structure coupling parameter and physically represents the ratio of the mass of the fluid to the mass of the structure per unit length of the waveguide. The functions f_1, f_2, f_3, f_4 and p represent the uncoupled wave solutions. The roots of $f_1 = 0$ represent the in vacuo structural wavenumbers. The roots of $f_2 = 0$ represent the cut-on wavenumbers of a rigid-acoustic duct. In other words, this wavenumber originates when the structure is completely rigid. The solution of $p = 0$ is the acoustic plane wave. In some cases, the waveguide configuration is

such that the only plane wave possible is that of zero amplitude. The roots of $f_3 = 0$ represent the cut-on wavenumbers of the pressure-release acoustic duct where the structural boundary is perceived as a free surface by the acoustic fluid. Lastly, the roots of $f_4 = 0$ give the structural wavenumbers corresponding to $\mu = \infty$. These solutions turn out to be longitudinal and torsional wavenumbers for cylindrical shell systems. These waves, unlike the transverse flexural waves couple with the acoustic fluid through the Poisson's ratio. The functions f_1, f_2, f_3, f_4 and p are different for different geometric configurations. Their form for the individual geometries will be presented below.

The parameter μ causes the coupling between the structural and acoustic waves depending on its magnitude. For $\mu = 0$, the solution to Eq. (1) gives the structural waves $f_1 = 0$, the rigid duct cut-ons $f_2 = 0$ and the acoustic plane wave $p = 0$. Thus, for small μ, we get coupled waves that are perturbations to the above waves. Similarly, for large μ one gets perturbations to solutions of $f_3 = 0$ and $f_4 = 0$. This is evident from the equation itself. For various geometries, the Eq. (1) takes a specific form and its solution is the coupled wavenumber solution. These coupled wavenumbers have been found for the different geometries and for small and large fluid-coupling (μ) values using asymptotic methods by Sarkar and Sonti (2007a,b,c,d, 2009a,b) and Kunte, Sarkar, and Sonti (2010). In addition, in all these geometries, for large values of μ, Eq. (1) has a coupled wave solution that is not intuitively evident and also cannot be obtained through asymptotic methods. It has to be obtained only numerically and we shall refer to it as the 'numerical branch'. Only the schematic of the solutions to Eq. (1) is shown in Fig. 2 which has the uncoupled solutions also. This schematic captures the behavior of all structural acoustic waveguides that can be represented by Eq. (1). In the light of Eq. (1) and Fig. 2 we intend to highlight the common behavior of all the above systems in one document.

The article is organized as follows. In section 2, we consider a general infinite flexible structural acoustic waveguide and derive, with some rigor, the coupled dispersion relation in the generic form. In the following sections, we consider a few geometries to illustrate this. In section 3, we discuss the rectangular waveguide mentioned above, with the two boundary conditions, and show that the coupled dispersion relations conform to Eq. (1). Using the rectangular waveguide as the representative system, the common features of all the waveguides will be presented in detail. In section 4, we will present the coupled dispersion relations of the circular cylindrical shell. Here, the dispersion equation is derived for a general circumferential order n using the Donnell-Mushtari shell theory. Also, we specialize the general equation for the axisymmetric and the beam modes. In all these cases, the coupled dispersion equation has the form of Eq. (1), thus making the discussion in

section 1 equally relevant here also. Finally, in section 5, the coupled dispersion equation for the elliptical cylindrical shell is presented. The dispersion relation for the elliptical shell is based on the shallow shell theory which is a simplified shell theory as presented by Soedel (2000). Hence, for clarity, we will initially present the dispersion relation for a circular cylindrical shell (for a general n) using the shallow shell theory and then extend it to the elliptical shell. At appropriate places, specific details such as the nondimensional parameters for the relevant geometry will be mentioned.

Additionally, in keeping with the spirit of unifying the dispersion results obtained in the case of various geometries, we discuss the reduction of the governing equation for the fluid-filled elliptical waveguide to that for a circular cylindrical waveguide in a separate appendix. Such a simplification while being non-trivial, has not come to our notice in the literature.

Throughout the article, we shall denote the dimensional frequency by ω, the dimensional wavenumber by k_x, the fluid density by ρ_f. For the rectangular waveguide, the nondimensionalization has been done with respect to the coincidence conditions (ω_c is the coincidence frequency and k_c is the coincidence wavenumber). Thus, we have the non-dimensional frequency $\Omega = \omega/\omega_c$, the non-dimensional wavenumber $\xi = k/k_c$, the non-dimensional fluid loading parameter $\mu = \rho_f a/m$ (where m is the mass per unit area of the plate) and the non-dimensional fluid column height as $\lambda = k_c a$, where a is the dimensional fluid column height.

For the cylindrical geometry, Ω is the non-dimensional frequency given by $\omega a/c_L$, where a is the shell radius and c_L is the longitudinal wave speed in the material. $\kappa = k_x a$ is the non-dimensional wavenumber.

We clarify our terminology here. When we talk of a “coupled flexural wavenumber", what we mean is a flexural in vacuo wavenumber (or an uncoupled flexural wavenumber) that has been perturbed due to fluid loading. Thus, the words uncoupled and in vacuo are equivalent descriptions. In other words, the coupled flexural wavenumber is a dominantly flexural wavenumber (or dominantly the in vacuo/uncoupled flexural wavenumber) but with perturbations due to the fluid loading. The word “coupled" immediately implies the influence of the neighboring medium, i.e., structure for the acoustic wave and the fluid for the structural wave.

2 A general fluid-loaded waveguide

In a generalized three-dimensional orthogonal coordinate system, the equations of motion for a fluid-loaded structure can be written in the matrix form as

$$[\mathbf{L}]\{\mathbf{U}\} = \{\mathbf{0}\},$$

where $\{\mathbf{U}\}$ is the vector of displacement amplitudes and the matrix $[\mathbf{L}]$ is as defined below.

$$\begin{bmatrix} \mathbf{L}_{11} & \mathbf{L}_{12} & \mathbf{L}_{13} \\ \mathbf{L}_{21} & \mathbf{L}_{22} & \mathbf{L}_{23} \\ \mathbf{L}_{31} & \mathbf{L}_{32} & \mathbf{L}_{33}+\mathscr{F} \end{bmatrix} \begin{pmatrix} \mathbf{U}_1 \\ \mathbf{U}_2 \\ \mathbf{U}_3 \end{pmatrix} = \begin{pmatrix} 0 \\ 0 \\ 0 \end{pmatrix}, \tag{2}$$

where $\mathscr{F}$ is the fluid-loading term. $\mathbf{U}_1$ and $\mathbf{U}_2$ are the amplitudes of the displacement components in the two tangential directions while $\mathbf{U}_3$ is the amplitude in the normal direction.

The fluid-loading term $\mathscr{F}$ is equivalent to the pressure acting at the wall-surface modulo a constant. Since we are only interested in the form of the term, the exact constant is unimportant. Thus, using Euler's equation at the surface of the wall, we have

$$\left.\frac{\partial p}{\partial n}\right|_{\text{at wall}} = \rho_f \omega^2 U_3. \tag{3}$$

where $\frac{\partial p}{\partial n}$ is the gradient of the pressure in the normal direction and the pressure and displacement are assumed to be time-harmonic with a frequency ω. Let the pressure p be written as $p = P\mathbf{p}$, where P is the pressure amplitude while $\mathbf{p}$ contains the functional dependence on the spatial coordinates. Thus, Eq. (3) becomes,

$$\begin{aligned} P\left.\frac{\partial \mathbf{p}}{\partial n}\right|_{\text{at wall}} &= \rho_f \omega^2 U_3, \text{ or,} \\ P &= \frac{\rho_f \omega^2}{\left.\frac{\partial \mathbf{p}}{\partial n}\right|_{\text{at wall}}} U_3. \end{aligned} \tag{4}$$

Thus, the complete fluid-loading term $\mathscr{F}U_3$ is given by,

$$\begin{aligned} \mathscr{F}U_3 = p|_{\text{at wall}} &= P\mathbf{p}|_{\text{at wall}}, \\ &= \frac{\rho_f \omega^2 \mathbf{p}|_{\text{at wall}}}{\left.\frac{\partial \mathbf{p}}{\partial n}\right|_{\text{at wall}}} U_3, \text{ or,} \\ \mathscr{F} &= \frac{\rho_f \omega^2 \mathbf{p}|_{\text{at wall}}}{\left.\frac{\partial \mathbf{p}}{\partial n}\right|_{\text{at wall}}}. \end{aligned} \tag{5}$$

From Eq. (2), the determinant of the matrix $[\mathbf{L}]$ gives the coupled dispersion relation. After suitably non-dimensionalizing this equation and defining a fluid-loading

parameter μ, the equation can be now be written in the most general form as,

$$\begin{aligned}&(\text{In vacuo dispersion relation}) + \mathbf{F}\mu \left(\frac{\mathbf{p}\big|_{\text{at wall}}}{\left.\frac{\partial \mathbf{p}}{\partial n}\right|_{\text{at wall}}} \right) (\mathbf{L}_{11}\mathbf{L}_{22} - \mathbf{L}_{12}\mathbf{L}_{21}) = 0, \text{ or,} \\ &\underbrace{(\text{In vacuo dispersion relation})}_{f_1} \underbrace{\left(\left.\frac{\partial \mathbf{p}}{\partial n}\right|_{\text{at wall}} \right)}_{f_2 p} + \mathbf{F}\mu \underbrace{\left(\mathbf{p}\big|_{\text{at wall}}\right)}_{f_3} \underbrace{(\mathbf{L}_{11}\mathbf{L}_{22} - \mathbf{L}_{12}\mathbf{L}_{21})}_{f_4} = 0,\end{aligned} \tag{6}$$

where $\mathbf{F}$ is a constant.

$(\mathbf{L}_{11}\mathbf{L}_{22} - \mathbf{L}_{12}\mathbf{L}_{21})$ is the determinant of the first 2x2 sub-matrix in Eq. (2) and setting this term to zero gives back the tangential wavenumbers approximately since these displacements are still coupled to the normal displacement through the Poisson's ratio. The terms f_2 and p can be separated on evaluation of the derivative term for a particular geometry.

3 The two-dimensional rectangular waveguide

As shown in Fig. (1a), a two dimensional structural acoustic waveguide consists of a flexible plate loaded with a finite fluid column. There are two possible boundary conditions applicable at the top surface of the fluid, namely:- (a) y-directional acoustic velocity $v_y(x,a) = 0$, (b) acoustic pressure $p(x,a) = 0$. The non-dimensional coupled dispersion equations for these cases are given by

$$\overbrace{\left[\frac{\xi^4}{\Omega^2} - 1\right]}^{f_1} \left[\overbrace{\lambda\sqrt{\Omega^2 - \xi^2}}^{p} \overbrace{\sin\left(\lambda\sqrt{\Omega^2 - \xi^2}\right)}^{f_2} \right] + \mu \overbrace{\cos\left(\lambda\sqrt{\Omega^2 - \xi^2}\right)}^{f_3} = 0, \tag{7a}$$

$$\underbrace{\left[\frac{\xi^4}{\Omega^2} - 1\right]}_{f_1} \left[\underbrace{\lambda\sqrt{\Omega^2 - \xi^2}}_{p} \underbrace{\cos\left(\lambda\sqrt{\Omega^2 - \xi^2}\right)}_{f_2} \right] - \mu \underbrace{\sin\left(\lambda\sqrt{\Omega^2 - \xi^2}\right)}_{f_3} = 0, \tag{7b}$$

respectively as presented by Sarkar and Sonti (2007a,d). The form of the equations shown above fits into the general equation (Eq. (1)). The terms f_1, f_2, f_3 and p are indicated with overbraces and underbraces. $f_4 = 1$ in this case.

In the equations above, consider the condition $\mu = 0$ (uncoupled case). In this case, $\xi = \sqrt{\Omega}$ is a solution, which corresponds to the in vacuo bending wavenumber of the plate. Further, for Eq. (7a), we get additional solutions of the form $\lambda\sqrt{\Omega^2 - \xi^2} = n\pi$, $n \in 0, 1, 2, \ldots$. Similarly, for Eq. (7b), we get solutions of the

form $\lambda\sqrt{\Omega^2-\xi^2}=(2n+1)\pi/2$, $n\in 0,1,2,\ldots$. These wavenumber branches correspond to the 'rigid-duct cut-on wavenumbers', where the flexible plate (at $y=0$) behaves as a rigid wall. Now, with $0<\mu\ll 1$, the solution to the equations (Eqs. (7)) will be perturbations to the wavenumber branches discussed above as shown earlier by Sarkar and Sonti (2007a,d).

For the other extreme value of $\mu=\infty$, we take the transformation $\mu'=1/\mu$ and consider $\mu'=0$ and continue with the perturbation method for the solution. The coupled dispersion equations (Eqs. (7)), rewritten in terms of μ' result in

$$\mu'\left[\frac{\xi^4}{\Omega^2}-1\right]\lambda\sqrt{\Omega^2-\xi^2}+\cot\left(\lambda\sqrt{\Omega^2-\xi^2}\right)=0, \tag{8a}$$

$$\mu'\left[\frac{\xi^4}{\Omega^2}-1\right]\lambda\sqrt{\Omega^2-\xi^2}-\tan\left(\lambda\sqrt{\Omega^2-\xi^2}\right)=0. \tag{8b}$$

With $\mu'=0$ we get solutions to $\lambda\sqrt{\Omega^2-\xi^2}=(2n+1)\pi/2$ and $\lambda\sqrt{\Omega^2-\xi^2}=n\pi$. These represent the pressure-release cut-ons wherein the plate acts like a free-surface with pressure set to zero. Hence, for $(0<\mu'\ll 1)$, the solutions are perturbations on these pressure-release cut-ons. However, as mentioned earlier, the numerical solution contains the coupled wave that is not intuitive and that cannot be found through a regular perturbation approach (this is the 'numerical branch'). This is because this branch does not have an uncoupled counterpart (found by setting $\mu=\infty$).

The schematic of the above solutions is shown in Fig. (2), where one can see the individual uncoupled flexural, rigid-duct/plane-wave cut on (RD) and the pressure release cut-on (PR) wavenumbers. The uncoupled flexural wavenumber intersects the uncoupled fluid wavenumbers. The coupled wavenumbers however, no longer hold such individual identities. They are perturbations to the above uncoupled wavenumbers smoothly transitioning from one uncoupled wavenumber to the other with increasing frequency. Except at the intersection of two uncoupled wavenumbers, in each frequency region, the coupled wavenumber primarily follows an uncoupled wavenumber (flexure, RD or PR wavenumber). It is also identified as the corresponding coupled wavenumber (for e.g., the coupled flexural wavenumber). This coupled wavenumber lies above or below the uncoupled curve depending on the loading (mass/stiffness) perceived by the fluid/structure due to the presence of the structure/fluid at that frequency. For example, when the uncoupled flexural wavenumber perceives the fluid as a mass loading, then the coupled solution stays above the uncoupled wavenumber (since the phase speed drops) and similarly when it perceives the fluid as stiffness, then it falls below the uncoupled wave (as the phase speed goes up). In between it passes through the uncoupled flexural branch intersecting with the uncoupled pressure release cut-on (see Sarkar

and Sonti (2007b) for details). If we follow a single coupled branch, for e.g., the second coupled branch (for small μ), it begins as a perturbation to a rigid duct wavenumber, transitions to a dominantly structural wavenumber and follows the next rigid-duct branch. For small μ, this branch is a perturbation to the in vacuo flexural wavenumber and the wavenumber of the rigid waveguide. With increasing μ, these perturbations increase until for large μ, the branch is better identified as a perturbation to the pressure-release cut-on wavenumber. Also seen in Fig. (2) is the 'numerical branch' (the dotted line) which lies above the flexural and the acoustic plane wave at low frequencies. This has to be obtained numerically.

The above discussion regarding Fig. (2) holds for all the different geometries presented here. The only exception is that for the circular and elliptical geometries, the fluid and the shell curves of a given circumferential order may intersect more than once. The nature of the intersection however remains the same. Thus, the schematic in Fig. (2) will be seen repeating in several places in the dispersion plots, although with a shift in the origin.

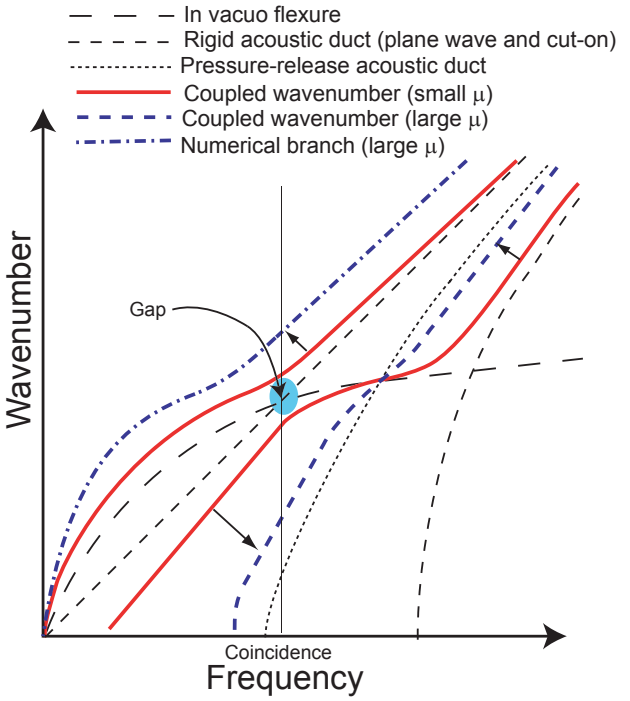

Figure 2: Schematic of the coupled wavenumber solutions. Arrows indicate transition of solutions from small μ to large μ.

4 The circular cylindrical shell

To obtain the dispersion equation of a circular cylindrical shell (of radius a, density ρ_s, shell thickness h, extensional wave speed c_L and Poisson's ratio ν) in the n^{th} circumferential mode, the equations of motion are first written in the matrix form as shown in Eq. (9) following Fuller and Fahy (1982).

$$\mathbf{L}\left\{\begin{array}{c} u_n \\ v_n \\ w_n \end{array}\right\} = \left\{\begin{array}{c} 0 \\ 0 \\ 0 \end{array}\right\}. \tag{9}$$

The elements of the matrix $\mathbf{L}$ are given by

$$\mathbf{L}_{11} = -\Omega^2 + \kappa^2 + \frac{1-\nu}{2}n^2,\ \mathbf{L}_{12} = \mathbf{L}_{21} = \frac{1}{2}(1+\nu)n\kappa,$$
$$\mathbf{L}_{13} = \mathbf{L}_{31} = \nu\kappa,\ \mathbf{L}_{22} = -\Omega^2 + \frac{1-\nu}{2}\kappa^2 + n^2,\ \mathbf{L}_{23} = \mathbf{L}_{32} = n.$$

The term $\mathbf{L}_{33}$ is given by

$$\begin{aligned} &-\Omega^2 + 1 + \beta^2\left(\kappa^2+n^2\right)^2 \text{ for in vacuo,} \\ &-\Omega^2 + 1 + \beta^2\left(\kappa^2+n^2\right)^2 - \frac{\Omega^2}{\chi}\left(\frac{\rho_f a}{\rho_s h}\right)\left[\frac{J_n(\chi)}{J_n'(\chi)}\right] \text{ with fluid.} \end{aligned} \tag{10}$$

In the above, $\chi = \sqrt{\Omega^2\left(\frac{c_L}{c_f}\right)^2 - \kappa^2}$, $\beta^2 = h^2/12a^2$ and u_n, v_n, w_n are the shell displacements in the longitudinal, circumferential and the radial directions, respectively. The term $\left(\frac{\rho_f a}{\rho_s h}\right)$ is defined as the fluid-loading parameter μ.

Setting the determinant of the above matrix $[\mathbf{L}]$ to zero gives the dispersion relation for a general circumferential order n. The dispersion relation is as follows :

$$\underbrace{\left[A_4\kappa^8 + A_3\kappa^6 + A_2\kappa^4 + A_1\kappa^2 + A_0\right]}_{f_1}\overbrace{\chi}^{p}\underbrace{J_n'(\chi)}_{f_2} + \mu\underbrace{\left[B_2\kappa^4 + B_1\kappa^2 + B_0\right]}_{f_4}\underbrace{J_n(\chi)}_{f_3} = 0. \tag{11}$$

where,

$$
\begin{aligned}
A_4 =&(-\beta^2+\nu\beta^2),\\
A_3 =&(-\nu\Omega^2\beta^2-4\beta^2n^2+3\Omega^2\beta^2+4n^2\nu\beta^2),\\
A_2 =&(-6n^4\beta^2-\nu\Omega^2+9\Omega^2\beta^2n^2-3n^2\nu\Omega^2\beta^2-2\Omega^4\beta^2-\nu^3+...\\
&\nu^2+\Omega^2-1+6n^4\nu\beta^2+\nu),\\
A_1 =&(-4n^6\beta^2-2\nu^2\Omega^2+\nu\Omega^4-\nu\Omega^2+2n^2\Omega^2-2n^2\nu\Omega^2-3n^4\nu\Omega^2\beta^2+...\\
&+4n^6\nu\beta^2-4\Omega^4\beta^2n^2-3\Omega^4+9\Omega^2\beta^2n^4+3\Omega^2),\\
A_0 =&(n^2\Omega^2-2\Omega^4+2\Omega^6-n^2\nu\Omega^2-2\Omega^4\beta^2n^4+n^8\nu\beta^2-n^4\nu\Omega^2+\Omega^2n^4+...\\
&n^2\nu\Omega^4+3n^6\Omega^2\beta^2-n^6\nu\Omega^2\beta^2-3n^2\Omega^4-n^8\beta^2),
\end{aligned}
$$

and

$$
\begin{aligned}
B_2 =&(1-\nu)\Omega^2,\\
B_1 =&(2n^2\Omega^2-3\Omega^4+\nu\Omega^4-2n^2\nu\Omega^2),\\
B_0 =&(\Omega^2n^4-n^4\nu\Omega^2-3n^2\Omega^4+n^2\nu\Omega^4+2\Omega^6).
\end{aligned}
$$

In the following sections, Eq. (11) will be simplified for two special cases, i.e., the axisymmetric mode ($n=0$) and the beam mode ($n=1$).

4.1 The axisymmetric mode ($n=0$)

From the expressions in Eqs. (9, 10), it is clear that for the axisymmetric mode (*viz.*, $n=0$), the circumferential vibration is uncoupled from the vibration in the other two directions. The radial and the longitudinal vibrations though are coupled. From Eq. (11), the coupled dispersion equation for the fluid-filled case is given by

$$
\begin{aligned}
|\mathbf{L}| = &\Bigg[\underbrace{\left(-\Omega^2+\kappa^2\right)\left(-\Omega^2+1+\beta^2\kappa^4-\frac{\nu^2\kappa^2}{\left(-\Omega^2+\kappa^2\right)}\right)}_{f_1}\overbrace{J_1(\chi)}^{f_2}\underbrace{\chi}_{p}\Bigg]+...\\
&...\Omega^2\mu\overbrace{J_0(\chi)}^{f_3}\underbrace{\left(-\Omega^2+\kappa^2\right)}_{f_4}=0.
\end{aligned}
\tag{12}
$$

Clearly, the equation above fits into the general equation (Eq. (1)) and the entire discussion on rectangular waveguides holds here also. In contrast to the rectangular waveguide, here the solution to $f_1=0$ gives the uncoupled longitudinal

wavenumber along with the uncoupled bending wavenumber. The resulting coupled longitudinal wave remains largely unaffected with increasing μ (and hence is part of the large μ solution also) in contrast to the flexural wave (which 'disappears' in the limit of $\mu = \infty$). The alternating mass and stiffness fluid-loading effect provided by the trigonometric terms sin() and cos() in the rectangular case are mimicked in this case by the Bessel functions J_0 and J_1. The only difference is in the adjustment of the scale and origin of the frequency axis. The difference in the non-dimensionalization scheme leads to a difference in the scale of the frequency axis between the present case and the two-dimensional waveguide system. Further, as the structural wave starts only beyond the ring frequency ($\Omega = 1$) the schematic figure in this case has the origin appropriately shifted as was noted by Sarkar and Sonti (2007c).

4.2 The beam mode ($n = 1$)

For $n > 0$, the off-diagonal terms of the matrix $\mathbf{L}$ become non-zero. Thus, the axial, radial and the circumferential vibrations are coupled. The dispersion relation is now significantly complicated. Hence, higher circumferential orders ($n > 0$) are in general better dealt with by scaling the frequency and the coupled wavenumbers in the high frequency or the low frequency regimes separately following Sarkar and Sonti (2009a). The dispersion relations for $n = 1$ in the high- and low-frequency cases are presented below and it is clear that these equations also conform to the general form (Eq. (1)).

4.2.1 The high frequency regime

The high frequency equation is given by

$$\underbrace{\left(-\Omega^2+\kappa^2\right)\left(-\Omega^2+\frac{1-\nu}{2}\kappa^2\right)\left(-\Omega^2+\beta^2\kappa^4\right)}_{f_1}\overbrace{\chi}^{p}\underbrace{J_1'(\chi)}_{f_2}-\ldots$$
$$\ldots\mu\Omega^2\underbrace{J_1(\chi)}_{f_3}\underbrace{\left(-\Omega^2+\kappa^2\right)\left(-\Omega^2+\frac{1-\nu}{2}\kappa^2\right)}_{f_4}=0. \tag{13}$$

The small μ case gives the longitudinal, the torsional, the flexural waves and the rigid-duct cut-ons. The plane wave solution is the trivial zero amplitude solution here, while the large μ results in the torsional wave, the longitudinal wave and the pressure release cut-ons. The torsional and the longitudinal waves are part of the large μ solution also since they are mostly unaffected by μ. As always, the 'numerical branch' is present here also.

4.2.2 The low frequency regime

The low frequency equation is given by

$$\underbrace{\left(-2\Omega^2+\kappa^4+\beta^2+4\beta^2\kappa^2-5\kappa^2\Omega^2\right)}_{f_1}\overbrace{\chi}^{p}\underbrace{J_1'(\chi)}_{f_2}-\ldots$$
$$\mu\Omega^2\underbrace{J_1(\chi)}_{f_3}\underbrace{\left[2\kappa^2-3\Omega^2+\kappa^4-3\kappa^2\Omega^2+1\right]}_{f_4}=0. \qquad (14)$$

The f_4 term represents complex wavenumbers that are longitudinal or torsional in nature. These waves do not cut on at low frequencies.

We have so far presented the equations of motion for fluid-filled cylindrical shells based on the Donnell-Mushtari shell theory. The last system we intend to discuss is the fluid-filled elliptical shell originally studied by Sarkar and Sonti (2009b). This system is based on the shallow shell theory. Hence, for a systematic transition, we present the shallow shell theory for the circular cylindrical shell in the following. In the next section, we then take up the elliptic case.

4.3 The higher order modes - Shallow Shell Theory

The shallow shell theory is a simplified shell theory that was originally developed for very thin shells. However, this theory can also be used for thin shells under certain loading conditions. In general, this theory is valid for higher order modes (with circumferential order $n \geq 2$).

In the shallow shell theory, the inertial terms in the axial and the torsional directions are neglected and an Airy's stress function is chosen such that the equations of motion in these two directions are automatically satisfied. Thus, from the equation of motion in the radial direction and the compatibility condition for the Airy's stress function ϕ, we now have two equations in the radial displacement component w and ϕ.

The coupled dispersion relation for the vibration of a fluid-filled circular cylindrical shell is given by eliminating ϕ from this system of equations and substituting the appropriate form (travelling wave) for w following Kunte, Sarkar, and Sonti (2010).

$$\overbrace{\left[\frac{\beta^2}{1-\nu^2}\left(n^2+\kappa^2\right)^4+\kappa^4-\Omega^2\left(n^2+\kappa^2\right)^2\right]}^{f_1}\underbrace{\chi}_{p}\overbrace{J_n'(\chi)}^{f_2}-\Omega^6c^4\mu\underbrace{J_n(\chi)}_{f_3}=0, \qquad (15)$$

which is also of the form given in Eq. (1). Thus, $f_4 = 1$ here as the longitudinal and torsional modes are eliminated by using the stress function approach.

In the following section we will present the dispersion relation for the elliptical cylindrical shell based on the shallow shell theory.

5 The elliptical cylindrical shell

The fluid-filled elliptical shell equations based on the shallow shell theory are a system of two equations in the radial displacement component w and the Airy's stress-function ϕ. The equations originally presented by Sarkar and Sonti (2009b) are as follows,

$$\begin{aligned}
&\left[\nabla^4 w - \left(\frac{1-\nu^2}{\beta^2}\right)\Omega^2 w - \left(\frac{1-\nu^2}{\beta^2}\right)\overline{p}\Big|_{\xi=\xi_0}\right](1-\varepsilon\cos(2\eta)) + \nabla_R^2\phi = 0,\\
&\nabla^4\phi(1-\varepsilon\cos(2\eta)) - \left(\frac{1-\nu^2}{\beta^2}\right)\nabla_R^2 w = 0,
\end{aligned} \tag{16}$$

where $\nabla^4 = \left(\frac{\partial^4}{\partial s^4} + 2\frac{\partial^4}{\partial s^2\partial\eta^2} + \frac{\partial^4}{\partial\eta^4}\right)$ and $\nabla_R^2 = \left(\frac{\partial^2}{\partial s^2}\right)$. s and η are the axial and the angular coordinates, respectively. ε is the eccentricity parameter and $\varepsilon = 0$ gives back the equations for the circular cylindrical shell. $\overline{p}$ is the dimensionless pressure. β is the thickness parameter defined here as $\beta^2 = h^2/12R^2$, where R is the mean radius of the shell. Eliminating ϕ from Eq. (16) and rearranging the terms,

$$\begin{aligned}
&\left[\left(\frac{\beta^2}{1-\nu^2}\nabla^8 w - \Omega^2\nabla^4 w\right) - \left(\frac{16\varepsilon\cos(2\eta)}{1-\varepsilon\cos(2\eta)}\right)\left(\frac{\beta^2}{1-\nu^2}\nabla^4 w - \Omega^2 w\right)\ldots\right.\\
&\qquad\left.+\frac{\nabla_R^4 w}{(1-\varepsilon\cos(2\eta))^2}\right] - \nabla^4\overline{p}\Big|_{\xi=\xi_0} + \left(\frac{16\varepsilon\cos(2\eta)}{1-\varepsilon\cos(2\eta)}\right)\overline{p}\Big|_{\xi=\xi_0} = 0,
\end{aligned} \tag{17}$$

where ξ is the radial coordinate and the shell surface is at $\xi = \xi_0$. The acoustic wave equation gives the dimensional pressure as

$$\nabla^4 p = \left(\frac{\omega^4}{c_f^4}\right)p = \left(\frac{\omega^4}{c_f^4}\right)\omega^2\rho_f b\left[\frac{Ce_m(\xi_0,q)}{Ce_m'(\xi_0,q)}\right]w,$$

where $Ce_m(\xi_0,q)$ are the modified Mathieu functions. A detail study of Mathieu functions can be found in the book by Gradshteyn and Ryzhik (2000). Following the same procedure as in the derivation of the fluid-filled circular cylindrical shell equations, we have

$$\nabla^4\overline{p} = \Omega^6\left(\frac{c_L}{c_f}\right)^4\mu\left[\frac{Ce_m(\xi_0,q)}{Ce_m'(\xi_0,q)}\right]w. \tag{18}$$

Thus, substituting the above relation into Eq. (17) we get

$$\left[\left(\frac{\beta^2}{1-\nu^2}\nabla^8 w-\Omega^2\nabla^4 w\right)-\left(\frac{16\varepsilon\cos(2\eta)}{1-\varepsilon\cos(2\eta)}\right)\left(\frac{\beta^2}{1-\nu^2}\nabla^4 w-\Omega^2 w\right)+\ldots\right.$$
$$\left.\ldots\frac{\nabla_R^4 w}{(1-\varepsilon\cos(2\eta))^2}\right]+\mu\left[-\Omega^6 c^4+\left(\frac{16\varepsilon\cos(2\eta)}{1-\varepsilon\cos(2\eta)}\right)\Omega^2\right]\left[\frac{Ce_m(\xi_0,q)}{Ce'_m(\xi_0,q)}\right]w=0, \tag{19}$$

which is in the standard form (Eq. (1)) used so far with

$$f_1=\left[\left(\frac{\beta^2\nabla^8 w}{1-\nu^2}-\Omega^2\nabla^4 w\right)-\left(\frac{16\varepsilon\cos(2\eta)}{1-\varepsilon\cos(2\eta)}\right)\left(\frac{\beta^2\nabla^4 w}{1-\nu^2}-\Omega^2 w\right)+\frac{\nabla_R^4 w}{(1-\varepsilon\cos(2\eta))^2}\right],$$
$$f_2 p=Ce'_m(\xi_0,q),$$
$$f_3=Ce_m(\xi_0,q),$$
$$f_4=1.$$

The equation above is strictly not a dispersion equation since it still contains terms with spatial dependences. An 'appropriate' form for w (for e.g., $w=\mathrm{e}^{\mathrm{i}\kappa s}(W_0+\varepsilon W_1\cos(2\eta))$) needs to be substituted (see the work by Sarkar and Sonti (2009b) for details) which then is operated upon by f_1. Then the method of harmonic balance needs to be used to find the dispersion equation. This dispersion equation carries the nominal cylindrical shell wavenumbers perturbed due to the shell eccentricity (ε) and due to the fluid loading. The $\cos(2\eta)$ term gets eliminated when the expansion is substituted in the equation above. Here again $f_1=0$ gives the in vacuo structural wavenumbers. Since the derivation of the shell equations is based on the shallow-shell theory, the structural term contains only the bending wavenumber. $f_2 p$ is the product of the rigid-duct acoustic cut-ons and the plane-wave term. In this case the two appear as a product but can be separated out when the derivative w.r.t. ξ, denoted by the $(')$ symbol, is evaluated. $f_3=0$ gives the pressure-release acoustic duct cut-ons. By setting $\varepsilon=0$, and using recurrence relations for Mathieu functions (Gradshteyn and Ryzhik (2000)) the above equation can be shown to reduce to Eq. (15), as shown in appendix A.

6 Conclusions

In this article, we show that the coupled dispersion equation of structural acoustic waveguides have a generic form where each of the terms (although different for each geometry) has the same physical interpretation. This is demonstrated using the rectangular, the circular cylindrical and the elliptical geometries. In the case of the elliptical waveguide (unlike the other cases), the coupled partial differential equation itself is put in the generic form. This is because the dispersion equation is too unwieldy to be presented here. The reduction of this partial differential equation to that for the circular cylindrical shell (also based on the shallow shell theory) is

discussed in a separate appendix. Also, the coupled wavenumber solutions of all the geometries are represented on a common schematic. This presentation brings out (despite geometrical differences) a unified understanding of how coupled waves are formed in structural-acoustic waveguides from their uncoupled wave counterparts.

References

Abramowitz, M.; Stegun, I. A. (1970): *Handbook of mathematical functions*. Dover Publications, Inc.

Fuller, C. R.; Fahy, F. J. (1982): Characteristics of wave propagation and energy distributions in cylindrical elastic shells filled with fluid. *Journal of Sound and Vibration*, vol. 81, no. 4, pp. 501–518.

Gradshteyn, I. S.; Ryzhik, I. M. (2000): *Table of Integrals, Series and Products*. Academic Press.

Kunte, M. V.; Sarkar, A.; Sonti, V. R. (2010): Generalized asymptotic expansions for the coupled wavenumbers in infinite fluid-filled flexible cylindrical shells. *Journal of Sound and Vibration*, vol. 329, pp. 5356–5374.

Lowson, M. V.; Baskaran, S. (1975): Propagation of sound in elliptic ducts. *Journal of Sound and Vibration*, vol. 38, no. 2, pp. 185–194.

Sarkar, A.; Sonti, V. R. (2007): An asymptotic analysis for the coupled dispersion characteristics of a structural acoustic waveguide. *Journal of Sound and Vibration*, vol. 306, pp. 657–674.

Sarkar, A.; Sonti, V. R. (2007): An asymptotic analysis for the coupled dispersion characteristics of a structural acoustic waveguide. In *Internoise 2007, Istanbul, Turkey, August 28-31, 2007*.

Sarkar, A.; Sonti, V. R. (2007): Asymptotic analysis for the coupled wavenumbers in an infinite fluid-filled flexible cylindrical shell : The axisymmetric mode. *Computer Modeling in Engineering and Sciences*, vol. 21, no. 3, pp. 193–207.

Sarkar, A.; Sonti, V. R. (2007): Coupled wavenumbers of an infinite plate loaded with a fluid column : An asymptotic approach. In *et al.*, I. V. R.(Ed): *Proceedings of National Symposium on Acoustics*, pp. 357–363. Macmillan India Pvt. Ltd.

Sarkar, A.; Sonti, V. R. (2009): Asymptotic analysis for the coupled wavenumbers in an infinite fluid-filled flexible cylindrical shell : beam mode. *Journal of Sound and Vibration*, vol. 319, pp. 646–667.

Sarkar, A.; Sonti, V. R. (2009): Wave equations and solutions of in-vacuo and fluid-filled elliptic cylindrical shells. *International Journal of Acoustics and Vibration*, vol. 14, no. 1, pp. 35–45.

Soedel, W. (2000): *Vibration of plates and shells*. Marcel-Dekker International.

Appendix A: Reduction of the elliptical shell equation to the circular cylindrical equation

As mentioned earlier, the development of the shell equations for the elliptical shell are based on the shallow shell theory. In the analysis of this problem, the elliptical cross-section has been treated as a perturbation on the circular cross-section and solutions are found in this limit. Thus, Eq. (19) can also be reduced to the shallow shell equation for the circular cylindrical shell as ε the measure of the eccentricity goes to zero. While it is easy to see that setting $\varepsilon = 0$ gives back the circular cylindrical equations for the structural terms the reduction of the fluid-loading term in this limit is non-trivial.

Thus, we consider only the fluid-loading term given by Eq. (18). The following coordinate transformation is used to convert from the rectangular Cartesian coordinate system to the elliptical coordinate system in the original reference by Lowson and Baskaran (1975), and later by Sarkar and Sonti (2009b)

$$\begin{aligned} x &= f\cosh(\xi)\cos(\eta), \\ y &= f\sinh(\xi)\sin(\eta), \end{aligned} \tag{20}$$

where $\xi \in [0,\infty)$ and $\eta \in [0,2\pi)$. Here, f is the x-coordinate of the focus of the ellipse given by ae (a is the semi-major axis and e is the eccentricity). $\xi =$ constant gives a family of ellipses of varying eccentricity (with semi-major and semi-minor axes ($f\cosh(\xi)$, $f\sinh(\xi)$), respectively). $\eta =$ constant gives a family of ellipses.

Following Sarkar and Sonti (2009b), the following term is defined,

$$q = \left(\frac{\omega^2}{c_f^2} - k_z^2\right)\frac{f^2}{2}.$$

As in the case of a circular cylindrical geometry, we define a radial wavenumber k_r as follows :

$$k_r = \sqrt{\frac{\omega^2}{c_f^2} - k_z^2}. \tag{21}$$

A separable solution to the wave equation in the elliptical coordinate system is chosen for the pressure. Thus, the two differential equations for the pressure terms

carrying the ξ and η dependencies are, respectively,

$$\frac{\partial^2 p_\eta}{\partial \eta^2} + \left(m^2 - q\cos(2\eta)\right) p_\eta = 0, \tag{22}$$

$$\frac{\partial^2 p_\xi}{\partial \xi^2} + \left(q\cosh(2\xi) - m^2\right) p_\xi = 0, \tag{23}$$

where m^2 is an arbitrary parameter. Substituting $q = 0$ in Eq. (22) and solving gives the circular cylindrical θ solution,

$$p_\eta = \cos(m\eta).$$

However, in Eq. (23), $q = 0$ and $\xi \to \infty, \cosh(\xi) \to \infty$ are the appropriate limits to obtain the governing equation for a circular cylindrical geometry and hence, no substitution is made initially. The solution for p_ξ is obtained in terms of the modified Mathieu elliptical functions, so that the final pressure solution is

$$p = Ce_m(\xi, q)\cos(m\eta)e^{ik_z z}.$$

The $Ce_m(\xi, q)$ term can be expanded as a series of Bessel functions with argument $(\sqrt{2q}\cosh(\xi))$, as noted by Lowson and Baskaran (1975). Reproducing Eq. (20.6.3) and Eq. (20.6.4) from Abramowitz and Stegun (1970) here,

$$\begin{aligned} Ce_{2r}(z, \frac{q}{2}) &= \frac{ce_{2r}\left(\frac{\pi}{2}, \frac{q}{2}\right)}{A_0^{2r}} \sum_{k=0}^{\infty} (-1)^k A_{2k}^{2r} J_{2k}(\sqrt{2q}\cosh(z)), \\ Ce_{2r+1}(z, \frac{q}{2}) &= \frac{ce'_{2r+1}(\frac{\pi}{2}, \frac{q}{2})}{\sqrt{q} A_1^{2r+1}} \sum_{k=0}^{\infty} (-1)^{k+1} A_{2k+1}^{2r+1} J_{2k+1}(\sqrt{2q}\cosh(z)) \\ &= \frac{ce_{2r+1}(0, \frac{q}{2})}{\sqrt{\frac{q}{2}} A_1^{2r+1}} \coth(z) \sum_{k=0}^{\infty} (2k+1) A_{2k+1}^{2r+1} J_{2k+1}(\sqrt{2q}\sinh(z)). \end{aligned} \tag{24}$$

The values of the coefficients in the above series can be found from the recurrence relations in Abramowitz and Stegun (1970). Reproducing the relations for even and odd subscripts, respectively,

$$\begin{aligned} &aA_0^{2n} - qA_2^{2n} = 0, \\ &(a - (2r)^2)A_{2r}^{2n} - q(A_{2r+2}^{2n} - A_{2r-2}^{2n}) = 0, \quad (r \geq 1) \end{aligned} \tag{25}$$

and

$$\begin{aligned} &(a - 1 - q)A_1^{2n+1} - qA_3^{2n+1} = 0, \\ &(a - (2r+1)^2)A_{2r+1}^{2n+1} - q(A_{2r+3}^{2n+1} - A_{2r-1}^{2n+1}) = 0, \quad (r \geq 1) \end{aligned} \tag{26}$$

where $a = m^2$. From the above equations, substituting $q = 0$, it can be seen that

$A_{2r}^{2n} = 0 \quad (m = 2n \neq 2r)$,

$A_{2r}^{2n} \neq 0 \quad (m = 2n = 2r)$,

and,

$A_{2r+1}^{2n+1} = 0 \quad (m = 2n+1 \neq 2r+1)$,

$A_{2r+1}^{2n+1} \neq 0 \quad (m = 2n+1 = 2r+1)$.

Considering the argument of Bessel's functions in Eq. (24), using Eqs. (20, 21),

$$(\sqrt{2q}\cosh(z)) = \sqrt{\left(\frac{\omega^2}{c_f^2} - k_z^2\right)} f \cosh(\xi). \Big|_{q\to 0,\ \xi\to\infty}$$
$$= \sqrt{\left(\frac{\omega^2}{c_f^2} - k_z^2\right)} r = (k_r r). \tag{27}$$

The same is true for the $(\sqrt{2q}\sinh(z))$ term in the second equation.

For the terms outside the summation,

for even $m = 2r$, $ce_{2r}\left(\frac{\pi}{2}, 0\right) = A_0^{2r}\cos\left(2r\left(\frac{\pi}{2}\right)\right) = A_0^{2r}(-1)^r$,

for odd $m = 2r+1$, $ce_{2r+1}(0,0) = A_1^{2r+1}\cos((2r+1)0) = A_1^{2r+1}$.

Also, $\lim_{\xi\to\infty}(\coth(\xi)) = 1$.

Substituting the above results in Eq. (24), we have,

$$Ce_{2r}(\xi\to\infty, \frac{q}{2}\to 0) = (-1)^r \sum_{k=0}^{\infty}(-1)^k A_{2k}^{2r} J_{2k}(k_r r),$$
$$Ce_{2r+1}(\xi\to\infty, \frac{q}{2}\to 0) = \frac{1}{\sqrt{\frac{q}{2}}}\sum_{k=0}^{\infty}(2k+1)A_{2k+1}^{2r+1}J_{2k+1}(k_r r), \tag{28}$$

or,

$$Ce_{2r}(\xi\to\infty, \frac{q}{2}\to 0) = (-1)^r \sum_{k=0}^{\infty}(-1)^k A_{2k}^{2r} J_{2k}(k_r r)\delta_{kr} = A_{2r}^{2r}J_{2r}(k_r r),$$
$$Ce_{2r+1}(\xi\to\infty, \frac{q}{2}\to 0) = \frac{1}{\sqrt{\frac{q}{2}}}\sum_{k=0}^{\infty}(2k+1)A_{2k+1}^{2r+1}J_{2k+1}(k_r r)\delta_{kr}$$
$$= \frac{1}{\sqrt{\frac{q}{2}}}(2r+1)A_{2r+1}^{2r+1}J_{2r+1}(k_r r), \tag{29}$$

where δ is the Kronecker delta function.

Differentiating Eq. (24) with respect to z and evaluating the results in the above limit, we have,

$$\begin{aligned} Ce'_{2r}(\xi \to \infty, \frac{q}{2} \to 0) &= \frac{1}{A_0^{2r}} A_{2r}^{2r} J'_{2r}(k_r r)(\sqrt{2q}\sinh(\xi)), \\ &= \frac{1}{A_0^{2r}} A_{2r}^{2r} J'_{2r}(k_r r)(k_r r), \\ Ce'_{2r+1}(\xi \to \infty, \frac{q}{2} \to 0) &= \frac{1}{\sqrt{\frac{q}{2}} A_1^{2r+1}} (2r+1) A_{2r+1}^{2r+1} J'_{2r+1}(k_r r)(\sqrt{2q}\sinh(\xi)), \\ &= \frac{1}{\sqrt{\frac{q}{2}} A_1^{2r+1}} (2r+1) A_{2r+1}^{2r+1} J'_{2r+1}(k_r r)(k_r r). \end{aligned} \tag{30}$$

Thus, using Eq. (30) in Eq. (18), the fluid-loading term, for both even and odd m, reduces to,

$$FL = \mu \frac{(1-\nu^2)}{\beta^2} \Omega^2 \frac{J_m(k_r r)}{(k_r r) J'_m(k_r r)} \overline{w}, \tag{31}$$

which is the same as that obtained in the circular cylindrical case as shown by Kunte, Sarkar, and Sonti (2010). The fluid-loading term is evaluated at the shell wall ($r = a$) when used to find the coupled wavenumbers.